A Tellurium Frequency Reference For Re-pumping During Laser-cooling of Strontium

By

Pakorn Wongwaitayakornkul

Advisor: Thomas Killian

A senior thesis submitted to the faculty of

William Marsh Rice University

In partial fulfillment of the requirement for the degree of

Bachelor of Science

Department of Physics and Astronomy

William Marsh Rice University

April 2013

Acknowledgements

I would like to thank to Dr. Thomas Killian for providing me the opportunity to work under his direction during this past academic year. He is not only a great advisor who always offers assistance whenever I asked or give a very carefully-read constructive comment during the process of writing this thesis, but he is also an excellent example of a researcher. His level of responsibility and hard work shows to me what it takes to be a great researcher. I also would like to thank Brian DeSalvo for his helps throughout the project. He is an incredible human resource who is always willing to answer my question, no matter how small or trivial that is.

Table of Contents

1. Introduction

Lasers are exceptionally powerful tools for preparing and studying atoms in specific states. One of the most exciting areas in physics today is the study of ultracold atoms, in which lasers play a significant role. With lasers, physicists are able to cool and trap atoms at temperatures as low as one millionth of a degree above absolute zero. During laser cooling, atoms can fall into states where they no longer interact with the lasers. As a result, they would be lost from the trap.. To resolve the problem, an additional laser can be added to the system to "repump" those atoms back into the cooling and trapping process. This thesis will describe the development of a new repumping system for laser-cooled strontium atoms using a laser operating at 481 nm. The project includes characterization of the new laser, construction of the temperature control system, and the spectroscopy of the tellurium cell.

This thesis will be organized as follow. In chapter 1, I will talk about the background and motivation of the project. I will describe the process of laser cooling and how it will be relevant to my project. Then I will explain energy levels of strontium and the problem that motivates this project. I will then describe some background of tellurium, which serves as a frequency reference for the repumping laser, and the procedure of performing spectroscopy on the tellurium molecules. Finally, the new 481-nm laser will be described. Chapter 2 is titled design and construction. I will describe the design and construction of the oven that heats up the tellurium cell and the temperature controller of the oven. In chapter 3, the application and result will be presented. I will show the data of the spectroscopy of tellurium absorption. Then I will describe the spectroscopy of the strontium repumping. Chapter 4 will conclude the whole project, discuss the viability of this method, and explain some errors of the data.

1.1 Laser Cooling

Laser cooling is a method for slowing atoms to low velocities using laser light. There are many different arrangements that have been developed in order to make this happen. In all of these strategies, atoms preferentially absorb photons with momenta that oppose the direction of the atom motion (Foot, 2005). Atoms then emit photons out in a random direction. As a result, the net momentum transfer causes the atoms to gradually become slower.

The simplest form of laser cooling is known as Doppler cooling. In the simple situation of laser-cooling in one dimension, it involves a two-level atom system as shown in Fig. 1 and two counterpropogating laser beams. By tuning the laser's frequency to be a bit below the resonance frequency for the transition (red-detuned), the Doppler shift will change the photon's frequency that moving atoms see making the atom absorb photons from the laser opposing motion. As a result of momentum conservation, atoms become slower in the laser's direction. There is a fundamental limit to how cold a sample of atoms can be cooled with Doppler cooling called the Doppler temperature. It can be expressed in terms of the decay rate of the population in the excited state (Γ), as $T_{\mathrm{Dop}} = \frac{\hbar\Gamma}{2k_B}$ (Phillips, 1992). For Sr, the Doppler temperature can be as low as $T_D \sim 1$ mK (X. Xu et al, 2003)

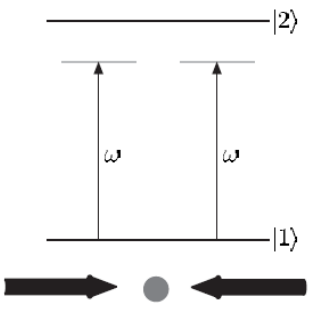

Figure 1: A system involves two of energy levels and two counterpropagating lasers |1> and |2> representing ground state and excited state respectively

This is a very powerful technique that can be generalized to other geometries and application. A single laser beam, opposing the directed motion of atoms in an atomic beam can cool and slow the atoms in the beam. This can be done by setting up the atomic beam to travel along the axis of a tapered solenoid. The varying magnetic field causes a Zeeman shift so as to counteract the changing Doppler-shift as atoms slow, so that atoms can remain in resonance with the fixed frequency of the laser. This slowing process is called Zeeman slowing.

Atoms in a gas move in all directions, and they can be cooled by the configuration of three orthogonal pairs of counter-propagating laser beam along the Cartesian axes, called 'optical molasses'. Fig. 2 illustrates optical molasses scheme as shown below.

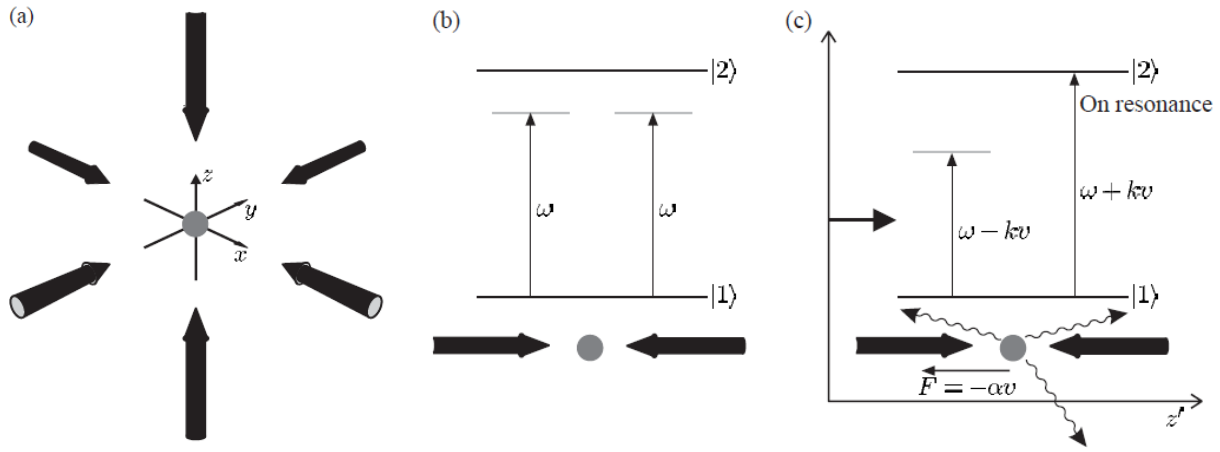

Figure 2: (a) Optical molasses scheme using three orthogonal pairs of counter-propagating laser beams along the Cartesian axes (b) A stationary atoms in a pair of counter-propagating laser beams experiences no resultant force. (c) The Doppler effect leads to more scattering of the light propagating in the direction opposite to the atom's velocity (Foot, 2005)

To this point, the schemes that are mentioned offer viscous damping in velocity space, in which the force is proportional to velocity for small velocities (H. J. Metcalf and Peter van der Straten, 1999). However, without trapping in the real space, atoms can diffuse and expand, and be lost. An additional restoring force must be added to the system to confine atoms in position.

This can be implemented by adding magnetic fields from magnet coils in anti-Helmholtz configuration. This causes a Zeeman shift in the atoms, which increases with the distance from the center of the trap. As the atoms move further from the center of the trap, their resonant frequency is shifted close to that of the laser. Therefore, they are more likely to recoil back toward the center of the trap by the photons. The direction of the recoil can be manipulated by the polarization of the lasers (E. L. Raab et al, 1987). This scheme is often called a magneto-optical trap (MOT). A cooled and confined cloud of atoms is a powerful experimental tool for understanding the behaviors of matter under this exotic condition. The laser-cooling configuration used in the experiment I will discuss is a MOT.

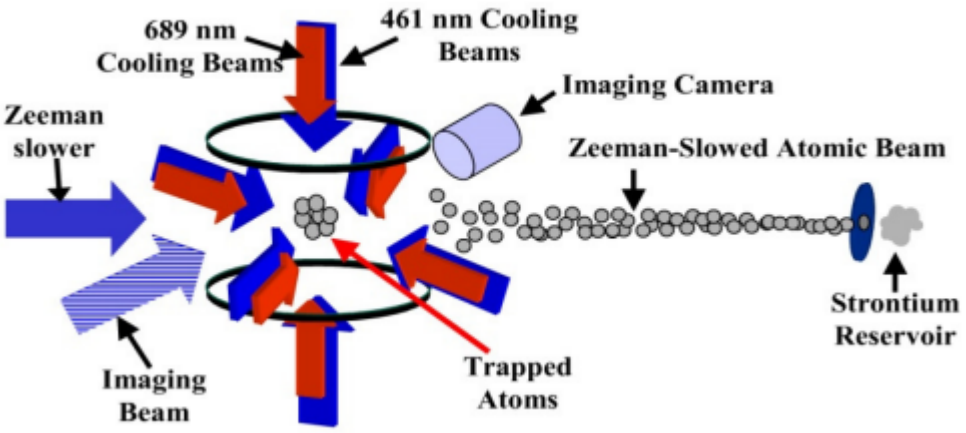

Figure 3: Schematic drawing of the experimental setup in Killian lab (Escobar, 2010)

1.2 Energy level of strontium

Elemental strontium was isolated in 1808 by Sir Humphrey Davy, who used electrolysis to do so. Its name comes from the Scottish town Strontian. Its atomic number is 38 and the ground state of neutral strontium is $1s^2 2s^2 2p^6 3s^2 3p^6 3d^{10} 4s^2 4p^6 5s^2\ {}^1S_0$ (J. E. Sansonetti and G. Nave, 2010). All laser cooling experiments in the Killian lab use strontium. One of the many things they study is Bose-Einstein Condensate (BEC) of the strontium (Escobar, 2010). BEC is a

state which a dilute gas of bosons cooled to temperatures near absolute zero. Getting a large fraction of bosons to occupy the lowest possible quantum state is one of the main challenges to reaching BEC (S. Stellmer et al, 2009), (X. Xu et al, 2003), (T. Kurosu and F. Shimizu, 1990), (T. Kurosu and F. Shimizu, 1992). At this point, quantum state effects are noticeable on a macroscopic scale. In order to do this, laser-cooling must work very efficiently. In Killian lab, several lasers are currently used to laser-cool the atoms. Figure 3 below illustrates relevant energy levels of the strontium.

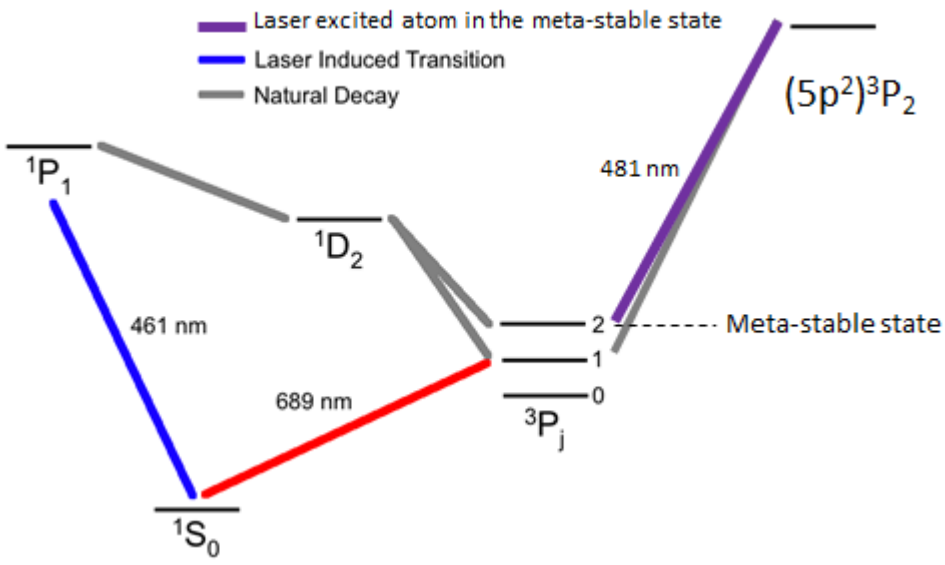

Figure 4: Energy levels of strontium with three lasers corresponding to the cooling process (Peron, 2012)

To laser cool and trap strontium atoms, the use of scattering force from photons is needed and therefore there are two possible cycling transitions, i.e. $^1S_0$-$^1P_1$ (461 nm) and $^1S_0$-$^3P_1$ (689 nm), as labeled in Fig. 4. Only $^1S_0$-$^1P_1$ transition will be our focus since laser cooling on this transition is the first stage of the cooling process, and it is the stage that needs a repumping laser. The problem with using this transition is that one in 10^5 $^1P_1$ atoms decays into $^1D_2$ level with the typical rate of $\gamma_P \approx (20\ \mathrm{ms})^{-1}$ (Escobar, 2010), (M. Yasuda and H. Katori, 2004). Then, atoms

in $^1D_2$ can naturally decay into either $^3P_1$ or $^3P_2$. The problem arises when strontium atoms naturally decay into $^3P_2$. Since the state has a relatively long life time, $\tau \sim 10$ minutes in the limit of zero temperature (M. Yasuda and H. Katori, 2004), (Derevianko, 2001), atoms in $^3P_2$ are stuck and will not decay to the ground state. Therefore, $^3P_2$ is often called a meta-stable state. In this state, the atoms no longer interact with 461 nm laser. Accordingly, an additional repumping system must be added to repump atoms in the metastable state back in the cycle.

Several repumping schemes have been used to repump the atoms in $^3P_2$ back to the ground state. A red 707 nm laser was used to access $^3S_1$ state (S. B. Nagel et al, 2003), (X. Xu et al, 2003). This scheme has a disadvantage because it requires an additional 679.2 nm laser because $^3S_1$ state can naturally decay to $^3P_0$ state, as illustrated in Figure 5. 707 nm is also an uncommon and difficult wavelength for diode lasers. So the diodes are expensive and short-lived. Therefore, the cost of having another laser and the complexity of the system to stabilize the additional laser are not so desirable.

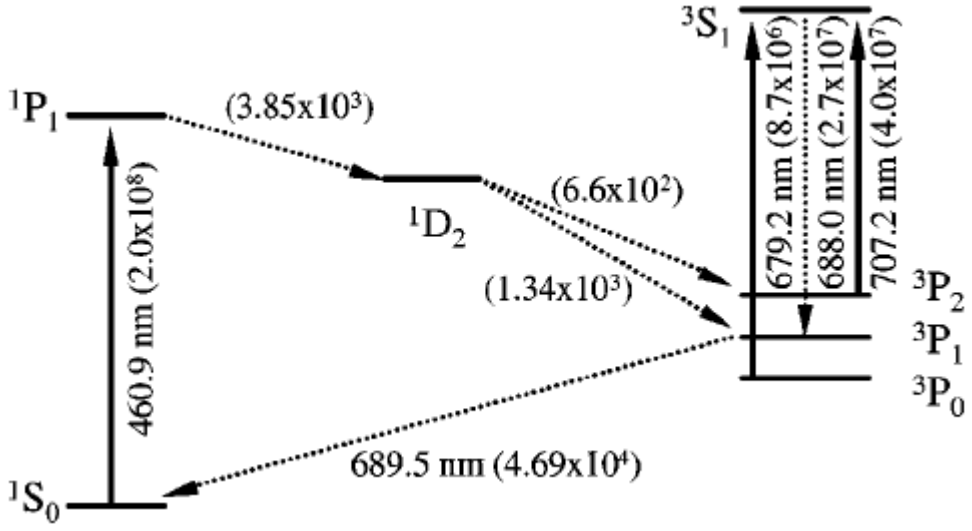

Figure 5: Strontium energy levels involved in the trapping of 3P2 atoms (S. B. Nagel et al, 2003)

A 497 nm light was also used to excite strontium atoms to (5s5d) $^3D_2$ state (N. Poli et al, 2005). For repumping leaking atoms back into blue MOT, they developed a laser source based on an antireflection coated laser diode stabilized in the Littrow extended cavity configuration, which delivers 25 mW at 994 nm. This light is frequency doubled on a 17-mm-long $KNbO_3$ crystal placed in a resonant cavity for improved conversion efficiency resulting in a 4 mW at 497 nm. The fact that 496-nm light involves second harmonic generation increases complexity and cost of the system.

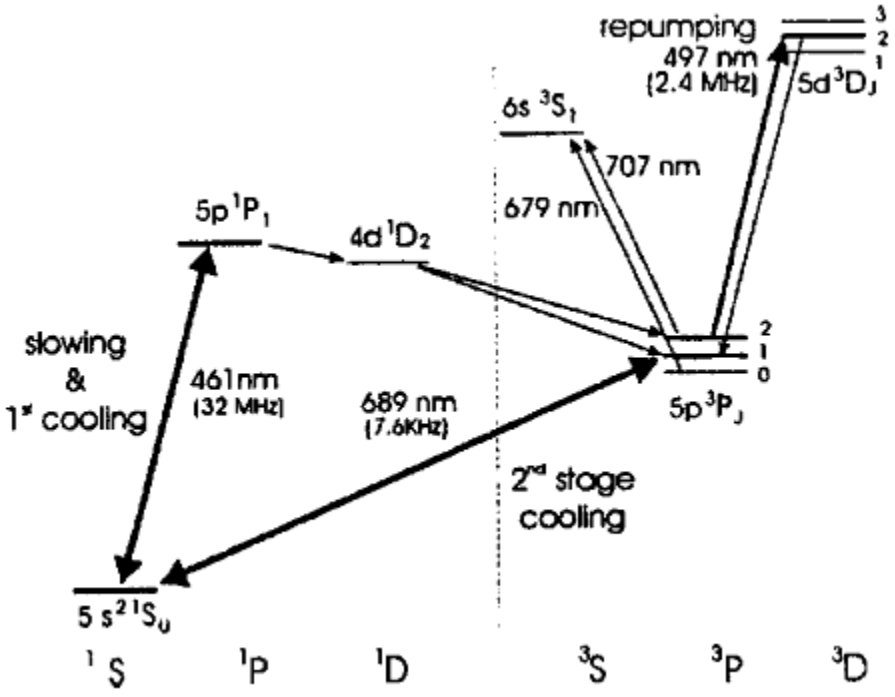

Figure 6: Relevant energy levels and optical transitions for laser cooling and trapping of strontium used in Poli's paper (N. Poli et al, 2005)

In Killian lab, the repumping scheme has been to utilize $^3P_2$-(5s4d) $^3D_2$ transition with 3012 nm laser (P. G. Mickelson et al, 2009). Lasers of this frequency range have just become available recently due to advances in nonlinear optics and fibre lasers. A 3012 nm laser has a historically difficult-to-reach wave length in the mid-infrared (MIR) and, thus, is costly.

Furthermore, this expensive laser can be used in other procedure in the lab, so my project is to help develop a new, cheaper method to repump strontium atoms out of $^3P_2$ state.

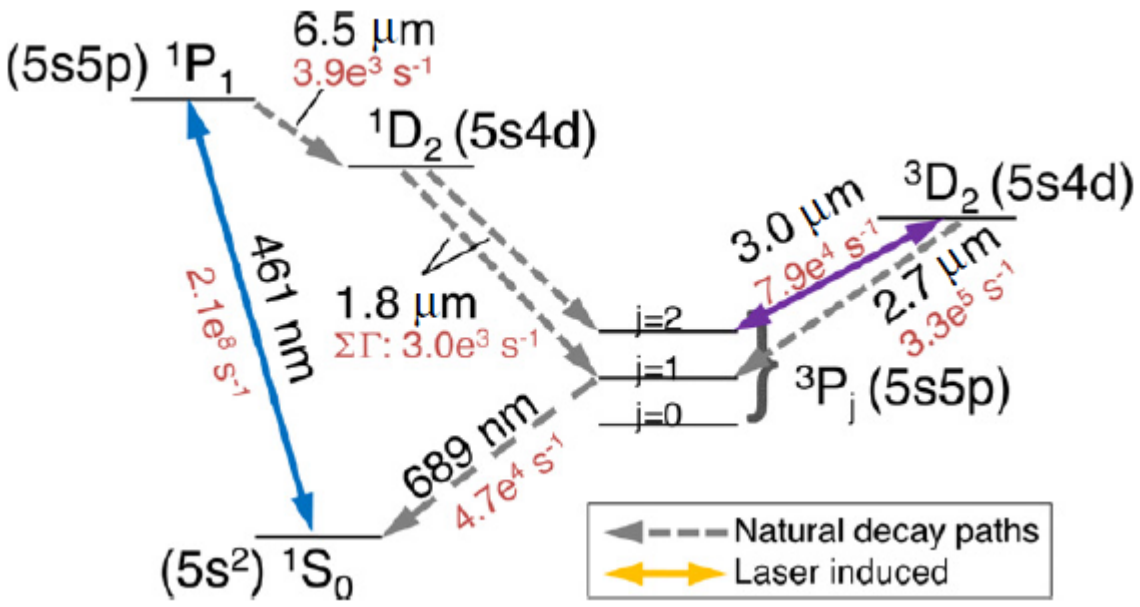

Figure 7: Strontium energy levels diagram associates with Mickelson's paper (P. G. Mickelson et al, 2009)

To tackle the problem cost-efficiently, a 481.3 nm diode laser is introduced to the setting for the repumping strontium atoms, via (5s5p) $^3P_2$-(5p^2) $^3P_2$ transition, as shown in Fig. 4, with wavenumber $k = 20776.087\ \text{cm}^{-1}$ (J. E. Sansonetti and G. Nave, 2010). With 481.3 nm laser, excited atoms in (5p^2) $^3P_2$ can naturally decay to either $^3P_2$ or $^3P_1$. From the $^3P_2$ state they are re-excited with the 481 nm laser. From the $^3P_1$ level, they decay back to the ground state and reenter the laser cooling cycle. Therefore, there are more atoms in the ground state and fewer atoms trapped in the metastable state. To execute this method, the laser requires a very stable and precise frequency. One of the challenges is finding a way to keep the laser on the right frequency. A common way to do this is to make a cell containing a gas of atoms or molecules that has a transition at the desired frequency. This serves as a reference frequency for the laser.

With electronics feedback locking system, one can lock the laser with a reasonably close frequency to the reference frequency of the gas in the cell.

It is difficult to use strontium for this for many reasons. One of the reasons is that only a small fraction of strontium gas can be prepared at $(5s5p)\,^3P_2$ level if $(5s5p)\,^3P_2$-$(5p^2)\,^3P_2$ transition is used. Fortunately, one of the atomic gas of tellurium's transition has wavenumber $k = 20776.0886\ \text{cm}^{-1}$, which is very close to that of $(5s5p)\,^3P_2$-$(5p^2)\,^3P_2$ transition of strontium $k' = 20776.087\ \text{cm}^{-1}$ (J. Carriou and P. Luc, 1980), (J. E. Sansonetti and G. Nave, 2010). Another reason why tellurium gas (Te_2) is a preferable choice is that there has been numerous works on the spectral line of tellurium (J. E. Sansonetti and G. Nave, 2010). Hence, an absorption spectroscopy of tellurium cell and a complimentary locking circuit can be used to stabilize and lock the 481 nm laser into an exact desired frequency.

The specifics of laser cooling and repumping can differ with isotope because of each isotope has a different excited frequency due to isotope shift (D. S. Hughes and C. Eckart, 1930). For example, Fig. 8 below illustrates the shifts of excitation frequency in $^3P_2$-$^3D_2$ transition of strontium for each isotope. The bosonic isotopes, ^{84}Sr , ^{86}Sr , and ^{88}Sr lack nuclear spin and hyperfine structure. ^{87}Sr has a very large nuclear spin $I = 9/2$ (Lide, 2008). This causes hyperfine splitting to its energy levels. Consequently, there are several sub-levels of meta-stable state, which complicated the repumping scheme.

1.3 Tellurium absorption spectroscopy

Tellurium was extracted first in 1782 from a gold ore by Austrian mineralogist F. J. Müller, but his discovery was forgotten until German chemist M.H. Klaproth recognized it as an element in 1798. The atomic number of tellurium is 52; its atomic weight is 127.60. It contains

of five stable isotopes: ^{120}Te (0.095%), ^{122}Te (2.59%), ^{124}Te (4.79%), ^{125}Te (7.12%), ^{126}Te (18.93%), and ^{130}Te (31.70%) (Berger, 1997). Because one of its energy gaps is close to our desired strontium transition as mentioned earlier, it can be used to stabilize the frequency of 481 nm laser for repumping strontium MOT by special frequency-offset locking technique (J. C. Hall and J. A. Magyar, 1976).

Absorption spectroscopy refers to techniques that measure the absorption of radiation, as a function of frequency or wavelength because the radiation interacts with a sample. The absorption varies with frequency of the radiation, giving an absorption spectrum. For a gas of atoms, Doppler broadening of spectral lines plays an important part in an absorption spectrum. Due to the Doppler Effect, the relationship between the angular frequency of radiation in the laboratory frame of reference (ω) and the angular frequency seen in a frame of reference moving at velocity $\vec{v}$ (ω') is given by $\omega' = \omega - \vec{k} \cdot \vec{v}$, where $\vec{k}$ is the wavevector of the radiation. From Maxwell-Boltzman distribution, the fraction of atoms in a gas with speed in the range v to $v + \mathrm{d}v$ is $f(v)\mathrm{d}v = \sqrt{\frac{M}{\pi 2k_B T}} \exp\left(-\frac{Mv^2}{2k_B T}\right) \mathrm{d}v$. If the Doppler Effect is taken into the account, the absorption function is given by $g_D(\omega) = \frac{c}{u\omega_0\sqrt{\pi}} \exp\left\{-\frac{c^2}{u^2}\left(\frac{\omega-\omega_0}{\omega_0}\right)^2\right\}$, where $u = \sqrt{2k_B T/M}$ is the most probable speed for atoms of mass M at temperature T and each atom absorbs radiation at frequency ω_0 in its rest frame (Foot, 2005).

1.4 481-nm laser

DL 100 is an external cavity diode laser in Littrow design. It contains micrometer screws allowing for coarse manual tuning. The laser resonator is thermally stabilized by means of a Peltier cooler, connected to the DTC 110 Diode Temperature Control. Ultra low noise operation of the laser is achieved by means of the Diode Current Control DCC 110 (Toptica tunable diode

laser, 2009). Our specifications include the wavelength of 481.3 nm, output power of 10.0 mW and mode hop free tuning of 20.0 GHz. It is able to sweep its frequency in a range of 479.3-487.4 nm with maximum output power of 15.3 mW. The laser is used to drive $(5s5p)\ ^3P_2$-$(5p^2)\ ^3P_2$ transition of strontium for re-pumping.

2. Design and construction

In this chapter, I will describe the design and construction of the equipment used for doing spectroscopy of tellurium gas and eventually for locking the repumping laser. Fig. 8 below displays the diagram of the set-up for doing spectroscopy. First, I will describe the construction of the oven and then the cell's temperature controller.

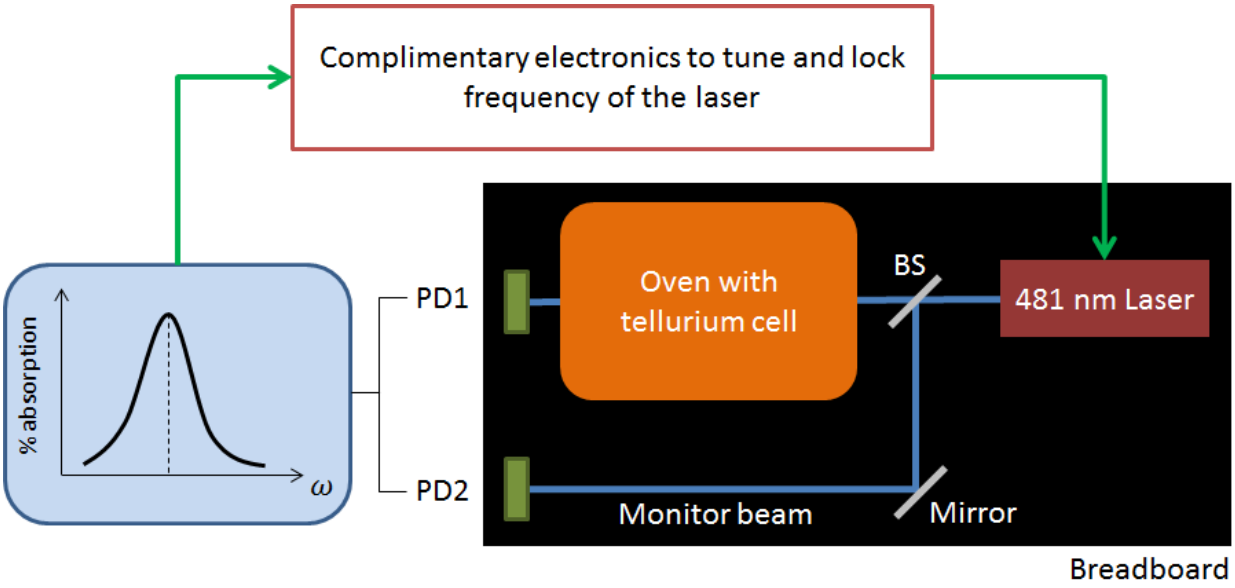

Figure 8: Illustration of the experimental setup

2.1 Oven

A Watlow ceramic fiber heater, with part No. VS102A06S, is used to assemble the oven for heating up tellurium cell (Ceramic Fiber Heaters). The heater can operate up to 1204℃, which is plenty to observe the absorption spectrum. Its maximum voltage across is 60 VAC. The tellurium cell is stuffed inside the heater using fiberglass. The heater is then installed inside an enclosure on the breadboard.

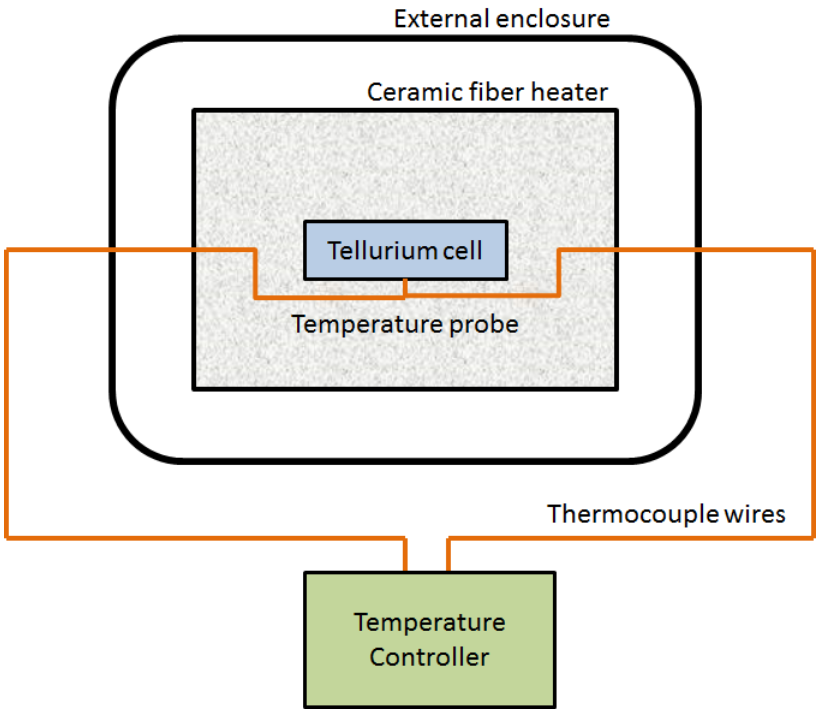

Figure 9: Oven setup

Fig. 8 illustrates the experimental set up. A 481 nm laser is sent through a beam splitter. One of the paths goes through the oven with tellurium cell and then is detected by photodiode 1. The other path is a monitor beam; therefore, it goes straight to photodiode 2. The signals from both photodiodes can be used to calculate the tellurium absorption spectrum at any temperature. The oven setup is demonstrated in Fig. 9. Together with the temperature controller, the experimental setup to do tellurium spectroscopy can be assembled as shown in figure 10 below.

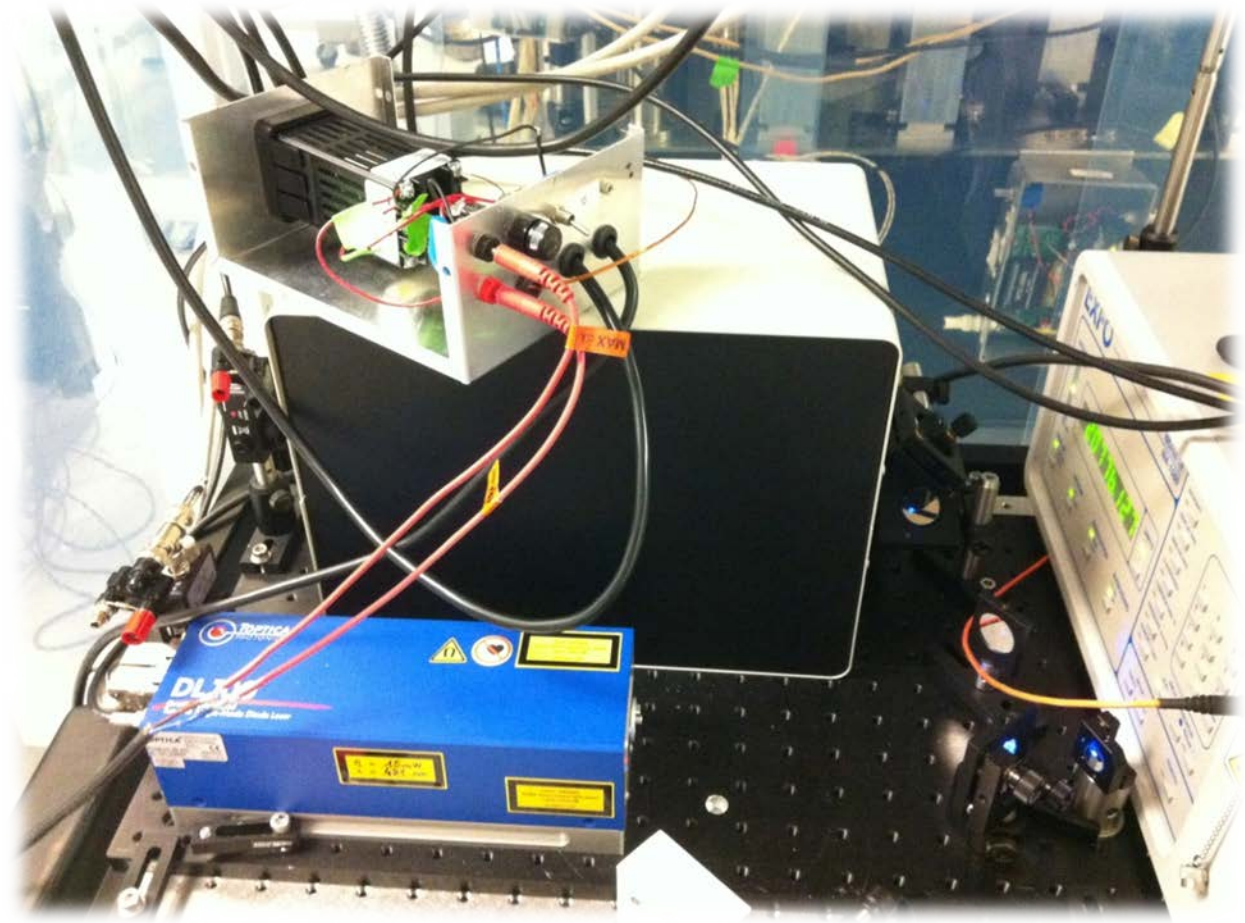

Figure 10: Experimental setup includes 481-nm laser, the tellurium cell oven and the temperature controller

2.2 Temperature controller

The shape of tellurium spectrum depends on the cell's temperature. An ability to control and steady the temperature of the cell is crucial to stabilize 481-nm laser frequency. Therefore, the temperature controller is assembled. Watlow temperature controller module and Watlow controls solid states relay are combined according to the Fig. 11 below.

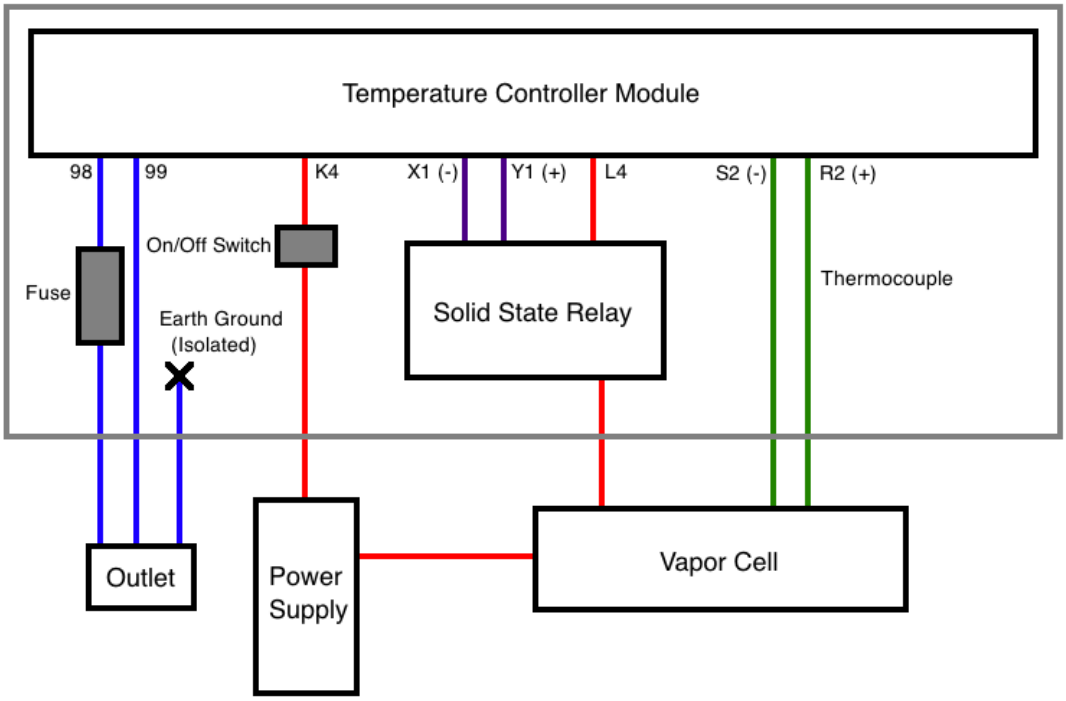

Figure 11: Diagram shows wire connections of the temperature controller (Peron, 2012)

The objective of the temperature controller is to regulate the temperature of the cell inside the oven. By measuring cell's temperature through thermocouple wires as shown in Fig. 9, the controller decide whether to feed current into the oven or to cut out the current. If the cell's temperature is below a particular set point, the controller keeps feeding the current into the oven. When the cell's temperature passes beyond a set point, the controller cut out the current. With this controller, the temperature of the cell can be regulated as fine as 1 °C.

Figure 12: (left) Watlow solid state relay (middle) Watlow temperature control module (right) Watlow ceramic fiber heater

Fig. 12 above shows images of the components of temperature controller and the oven. The finished temperature controller is shown in Fig. 13 below.

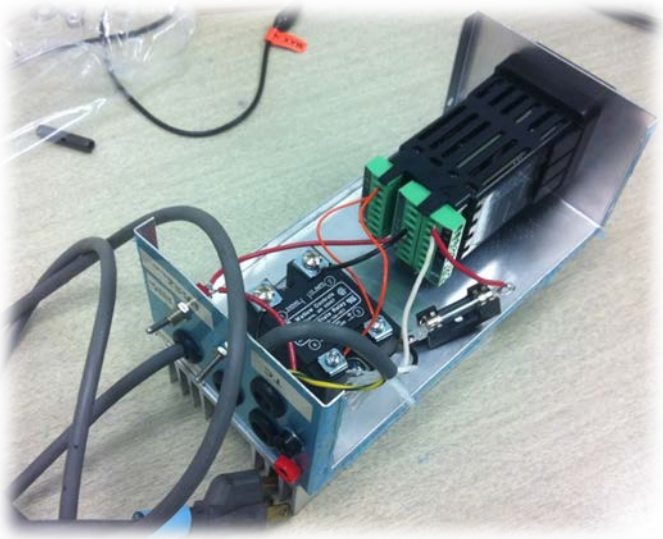

Figure 13: Finished temperature controller

3. Application

3.1 Spectroscopy of tellurium

Tellurium atoms consist of numerous energy levels (J. Carriou and P. Luc, 1980). As a result, its spectroscopy provides countless absorption lines. However, the exact structure of its energy level is unclear. Only the tellurium absorption lines that have the corresponding energy close to that of the $(5s5p)\ ^3P_2$-$(5p^2)\ ^3P_2$ transition of strontium will be discussed. The tellurium absorption lines we use are at about 20776.0 cm^{-1}. We observe several lines. It is reasonable to assume that all of these lines are a result of transitions between two electronic states and each electronic state consists of several sub-levels due to vibrational and rotational energy. For simplicity, we will assume that each line that we see originates from a distinct ground state.

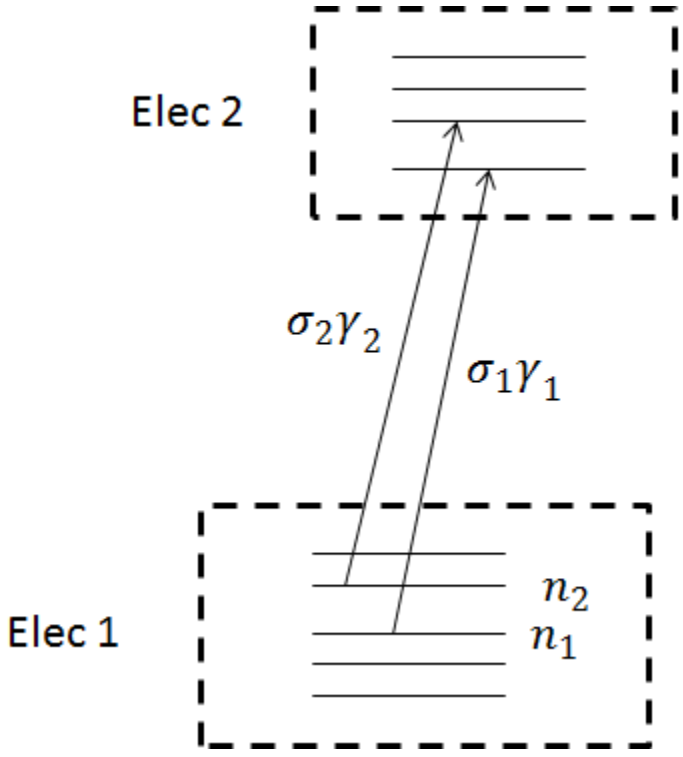

Figure 14: Diagram illustrating a model of tellurium energy

Fig. 14 above illustrates a model of tellurium energy where n_i, represent a density of molecules in state i, and σ_i, and γ_i are the absorption cross-section, and natural linewidth of the transition out of state i. With this model, the tellurium spectroscopy allows us to extract those variables out from equation fitting. However, with limited information, it is impossible to determine the values of each parameter. The best parameter extraction that can be achieved is to determine an absorption line characteristic parameter which is defined by the product of three variables above, i.e. $n_i\sigma_i\gamma_i$ for the ith absorption line.

From Beer's law, assuming that the tellurium gas is homogeneous, the transmitted intensity of the laser passing through the tellurium cell can be written as $I = I_0 e^{-nL\int_{-\infty}^{\infty} \mathrm{d}v_x f(v_x)\sigma(f,v_x)}$, where I_0 is the intensity of the laser with 100% transmission, n is the density of tellurium atoms in the states that interact with photons, L is the length of the cell and $\sigma(f, v_x)$ is an absorption cross-section as a function of laser frequency and velocity of the tellurium atoms in same direction as the laser's propagation. As shown below, two absorption lines are involved in the range of our interest. Therefore, based on this model, absorption cross-section can be expressed as

$$\sigma(f, v_x) = \frac{\sigma_1}{1+\left[\frac{2\left(f-f_1-\frac{v_x}{\gamma_1}\right)}{\gamma_1}\right]^2} + \frac{\sigma_2}{1+\left[\frac{2\left(f-f_2-\frac{v_x}{\gamma_2}\right)}{\gamma_2}\right]^2}.$$

The total absorption cross-section is the sum of the contribution from each absorption line. For each line, the absorption cross-section near resonance is given by a Lorentzian (Demtroder, 2008). Since in this case the Doppler broadening is much larger than the natural broadening, the Lorentzian functions can be treated as delta functions using the relation:

$\lim_{\gamma\to\infty}\frac{2\pi}{\gamma}\left(1+\frac{4x^2}{\gamma^2}\right)^{-1}=\delta(x)$ (Peron, 2012). After including the intensity background variation and delta-function approximation, the final expression for transmitted laser intensity is

$$I(k)=I_0(A+Bk)\exp\left[-\left(\frac{L\lambda}{2\pi}\sqrt{\frac{m}{2\pi k_B T}}\right)\left(n_1\sigma_1\gamma_1\exp\left[-\frac{m\lambda^2c^2(k-k_1)^2}{2k_BT}\right]\right.\right.$$

$$\left.\left.+\,n_2\sigma_2\gamma_2\exp\left[-\frac{m\lambda^2c^2(k-k_2)^2}{2k_BT}\right]\right)\right]\text{\_\_\_\_\_}(1)$$

After the experiment is set up according to Fig. 14, the spectroscopy of tellurium gas can finally be performed. At a specific temperature, the diode laser's wave number can be varied from 20776.0 to 20776.1 cm^{-1} by controlling the current feeding into the laser with increment of 0.005 cm^{-1}. The laser's intensity was measured in Volts, instead of Watts, because it is easier to read off from oscilloscope. Since the voltage across photodiode is proportional to the intensity of radiation onto photodiode and Beer's law only takes the ratio of the intensity into account, Volt will be a reasonable unit for intensity in our experiment. In this range, two absorption lines are expected, according to Carriou and Luc's literature. The spectroscopy was carried out at four different temperatures (400 ℃, 423 ℃, 448 ℃, and 473 ℃). Below is a superimposed plot of the spectroscopy at various temperatures.

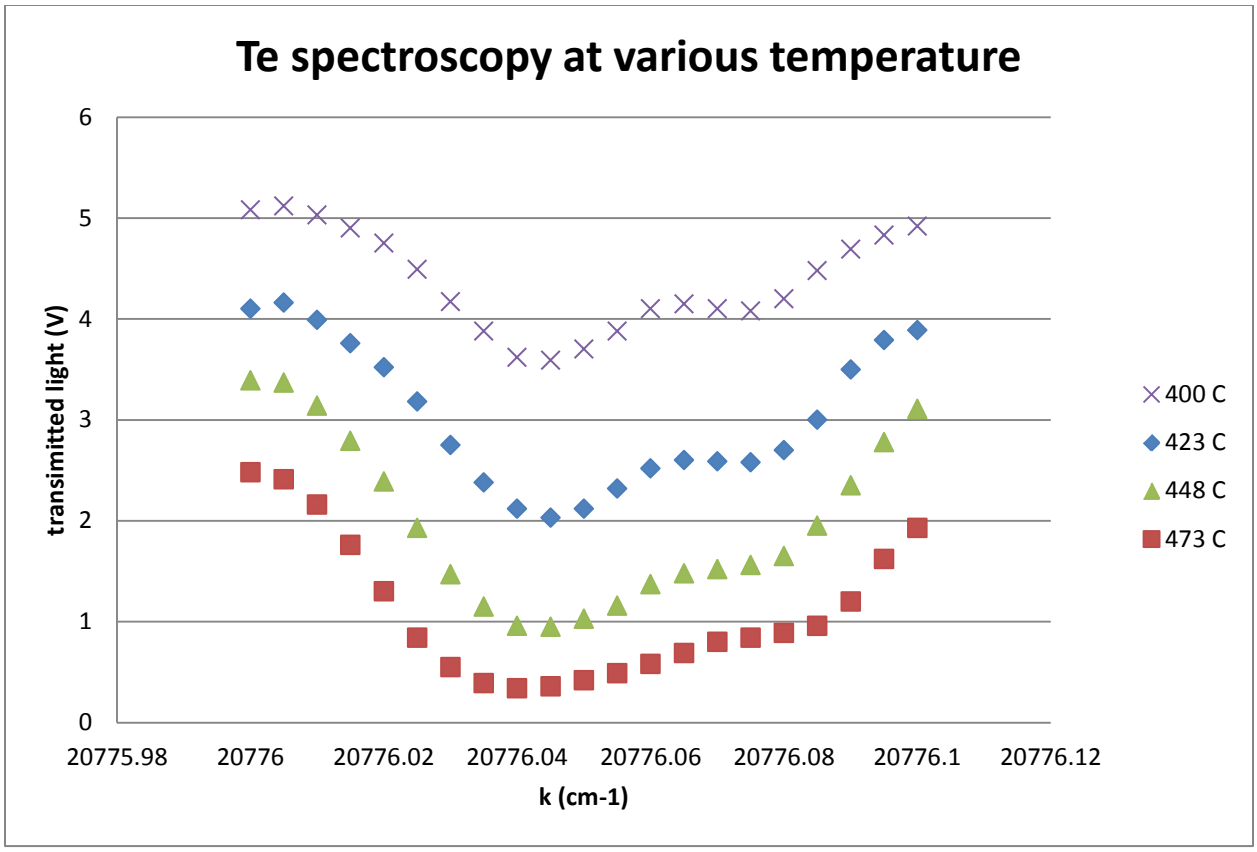

Figure 15: Tellurium spectroscopy at various temperatures

While recording the intensity of the laser passing through the tellurium cell at each temperature, the intensity of a monitor beam is also recorded to observe the change in the laser's intensity as its frequency is changed. Fig. 16 plots the data of the transmitted intensity versus laser's wavenumber for four temperatures, along with the linear fitting line. This best fitting line provides value A (slope) and B (y-intersection) in Eq. 1. From our data, A = 2.8000 V*cm and B = 5.1435 V.

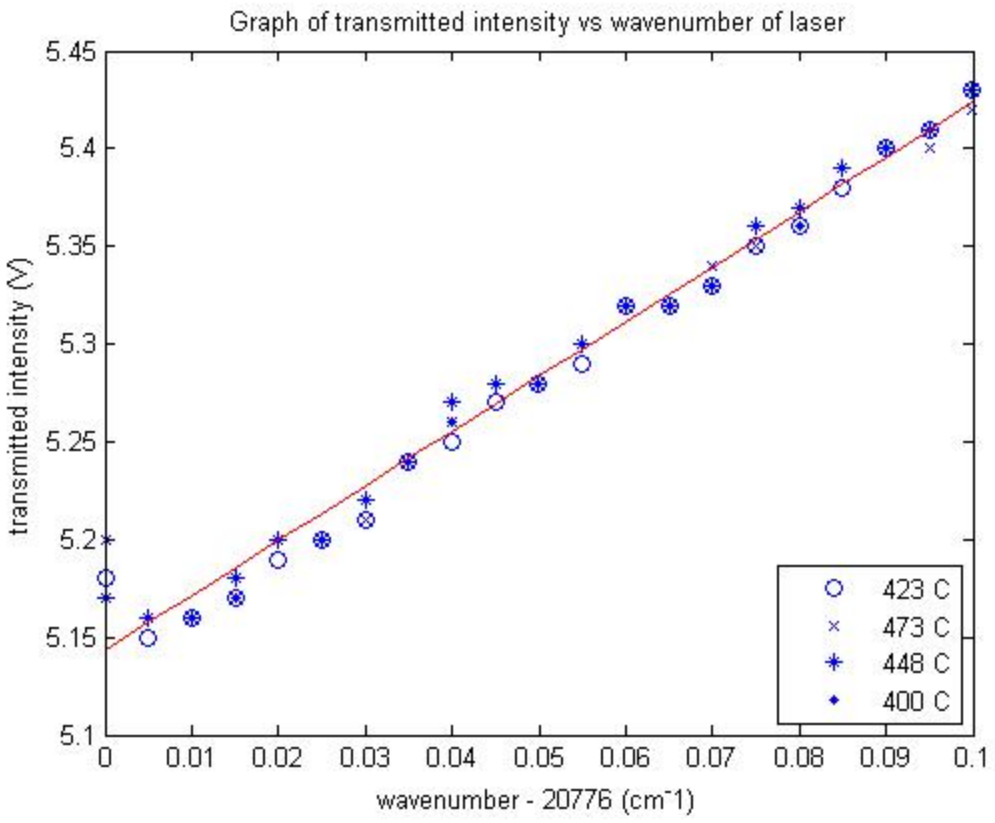

Figure 16: Graph of transmitted intensity vs laser's wavenumber

Lsqcurvefit, a Matlab function, is used to extract parameter from Eq. 1. The fitting function is defined as

$$F(\vec{x}, \vec{k}_0, k) = (B + Ak)\exp[-\sqrt{x_1}(x_2\exp[-x_1(k - k_1)^2] + x_3\exp[-x_1(k - k_2)^2])] \quad (2)$$

$\vec{x}$ and $\vec{k}_0$ are parameters to be extracted and k is an independent variable representing wavenumber of the laser. A and B are background parameters determined from Fig. 16. This defined function can be compared to Eq.1 to obtain physical meaning of each parameter:

$x_1 = \frac{m\lambda^2 c^2}{2k_B T}$, $x_2 = \frac{Ln_1\sigma_1\gamma_1}{2\pi c}$, and $x_3 = \frac{Ln_2\sigma_2\gamma_2}{2\pi c}$. k_1 and k_2 are resonant frequencies of absorption line 1 and 2 respectively. The result of parameter extraction work best for low temperature T = 400°C. Fig. 18 shows the data plot (red) with best fit curve (blue).

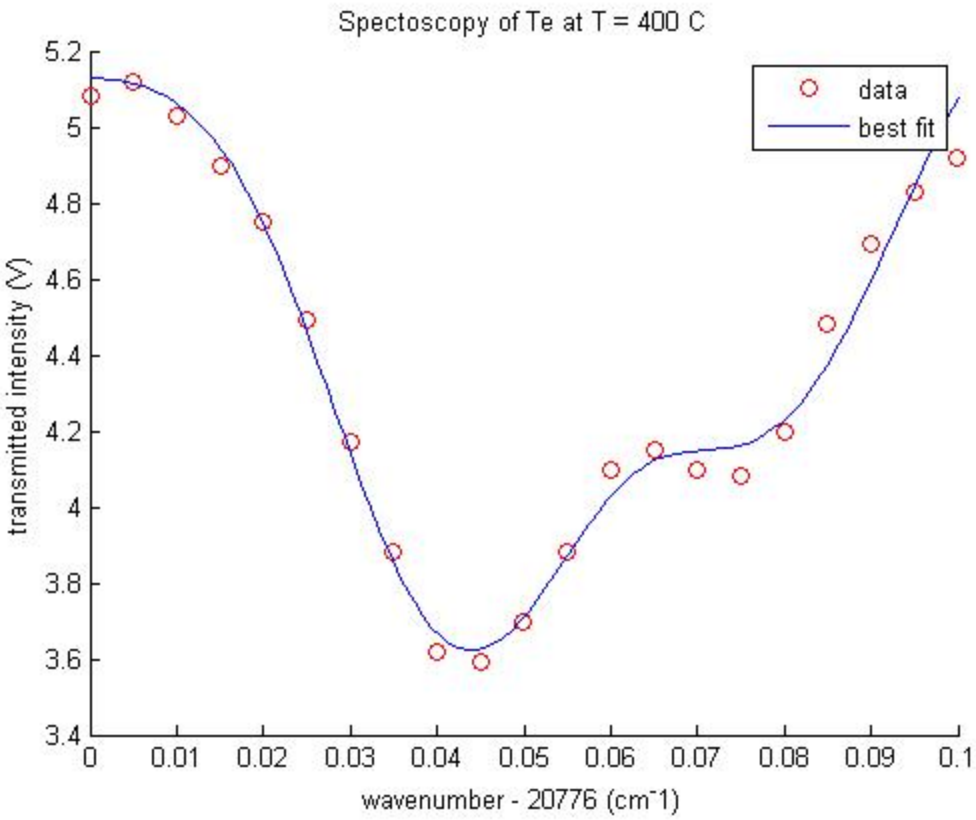

Figure 17: Spectroscopy of Te at low temperature (T = 400C) with best fit curve

From fitting the data at T = 400°C, $\vec{k}_0$ is determined to be $\vec{k}_0^* = (0.0432, 0.0780) + 20776\ \text{cm}^{-1}$. These two lines are expected as Carriou and Luc's data suggested that there should be two lines in our specific range with $\vec{k}_0' = (0.0609, 0.0886) + 20776\ \text{cm}^{-1}$ (J. Carriou and P. Luc, 1980). To improve our fitting, $\vec{k}_0$ will be fixed at our $\vec{k}_0^*$, the wavenumber decided by letting the center frequencies be variables in the fit of the low temperature data, at $(0.0432, 0.0780) + 20776\ \text{cm}^{-1}$ in the fitting plot of other temperature and only $\vec{x}$ will be varied.

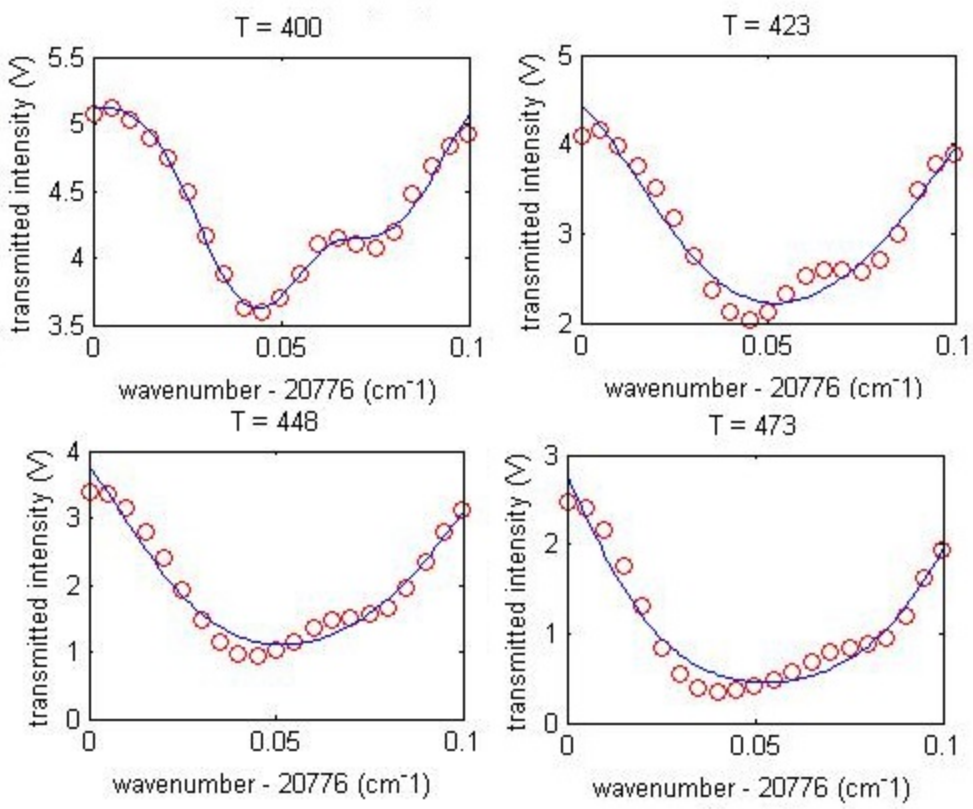

Figure 18: Curve fit of Te spectroscopy at various temperature

Fig. 18 shows the data and curve fit of Te spectroscopy graph at four different temperatures labeled in the titles. In this fitting, $\vec{x}$ is the varying variable. After these parameters are extracted, the temperature of the tellurium cell can be determined by x_1 from $T(x_1) = \frac{m\lambda^2 c^2}{2k_B x_1}$, where m is the mass of Te_2. The table below displays the value of $\vec{x}$ from parameter extraction at each temperature, with the according temperature determined by x_1.

T (°C)	x_1 ($\times 10^3$ m^2)	x_2 (m^{-1})	x_3 (m^{-1})	$T(x_1)$ (°C)
400	2.5584	0.0072	0.0045	976
423	0.8506	0.0235	0.0139	3483
448	0.7631	0.0451	0.0237	3914

473	0.6197	0.0751	0.0414	4883

The temperatures obtained from parameter x_1 are not quite in the range of our temperature measured by thermocouple wires. The possible causes of this will be explained more thoroughly in conclusion. Also if our assumption about the model is true, the characteristic parameter of the tellurium absorption line can be determined. Using the length of the cell L to be $L = 4 \text{ inches} = 0.1016 \text{ m}$. The characteristic parameter of each line $n_i\sigma_i\gamma_i$ can be determined from x_2 and x_3. The table below displays those values.

T (°C)	$n_1\sigma_1\gamma_1$ ($\times 10^8$ s/m)	$n_2\sigma_2\gamma_2$ ($\times 10^8$s/m)
400	1.331	0.841
423	4.352	2.574
448	8.365	4.403
473	13.918	7.716

3.2 Result of repumping strontium

The specifics of laser cooling and repumping can differ with isotope because of each isotope has a different excited frequency due to isotope shift (D. S. Hughes and C. Eckart, 1930). For example, Fig. 19 below illustrates the shifts of excitation frequency in $^3P_2$-$^3D_2$ transition of strontium for each isotope. The bosonic isotopes, ^{84}Sr , ^{86}Sr , and ^{88}Sr lack nuclear spin and hyperfine structure. ^{87}Sr has a very large nuclear spin $I = 9/2$ (Lide, 2008). This causes hyperfine splitting to its energy levels. Consequently, there are several sub-levels of meta-stable state, which complicated the repumping scheme.

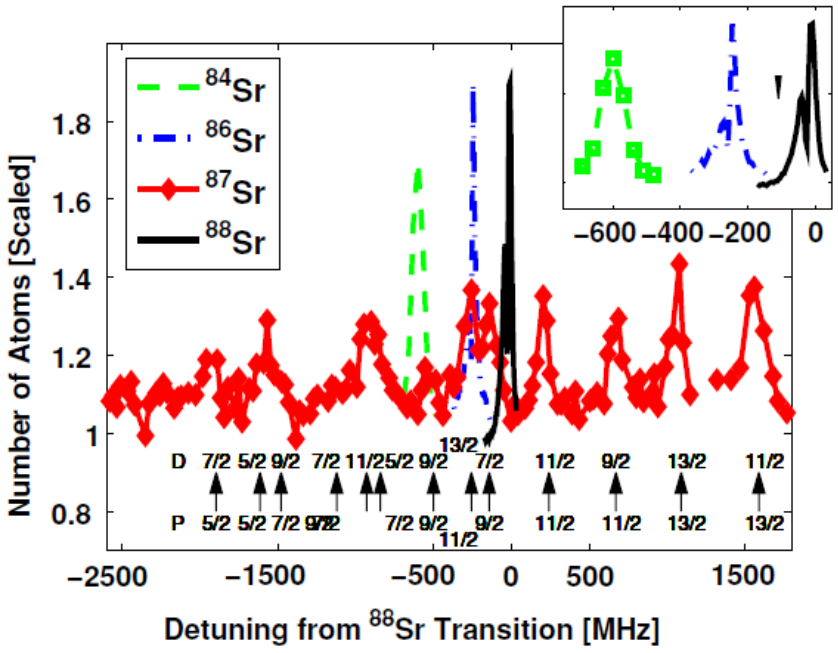

Figure 19: Spectroscopy of 3P2-3D2 transition of the strontium for different isotope (P. G. Mickelson et al, 2009)

As mentioned in the introduction, the strontium atoms are repumped into the MOT to create a certain state of strontium with number of trapped atoms as high as possible. Below are graphs of the number of atoms of strontium MOT as a function of the repumping laser's wavenumber (k), for isotope ^{86}Sr and ^{88}Sr.

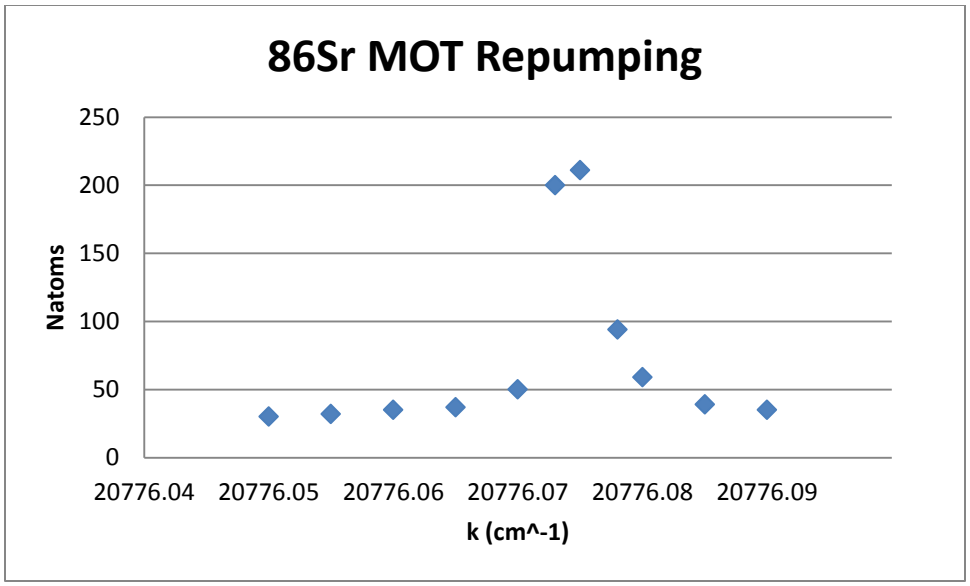

Figure 20: Graph of the number of atom trapped and frequency of the repumping laser for 86-Sr MOT

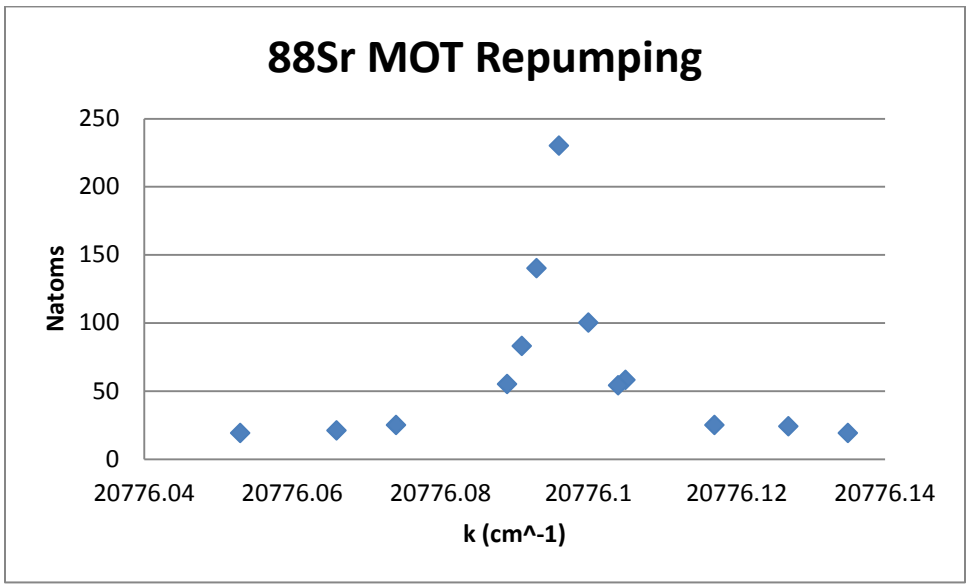

Figure 21: Graph of the number of atom trapped and frequency of the repumping laser for 86-Sr MOT

Fig. 24 and 25 show that the optimum wavenumber of the repumping laser of strontium MOT is around 20776.072 cm^{-1} for ^{86}Sr and 20776.095 cm^{-1} for ^{88}Sr. This is a promising result regarding the shape and location of our tellurium spectroscopy for locking these wavenumbers to the side of tellurium's Doppler broadening line.

4. Conclusion

The project demonstrates the potential of using tellurium as a frequency reference for repumping laser for cooling strontium atoms. The model of tellurium energy level was explored and the equipment was prepared to lock 481-nm laser. The result assures the viability of this scheme. Because it is less expensive and complicated to set up comparing to the other schemes mentioned in the introduction, using a single 481-nm to repump strontium atoms via $(5s5p)\,^3P_2$-$(5p^2)\,^3P_2$ transition is a promising solution to repump cooled strontium atoms in future research.

The spectroscopy of the tellurium seems to follow our model of the absorption. However, the graph fitting of the plots gives somewhat unreasonable result. By parameter extraction, the temperature of the cell can be determined. These values of temperature, though, do not match with the actual temperature of the cell measured by thermocouple wires. Some explanations to the result are as follow:

- The shifts in expected resonant wavenumber and the width of absorption spectrum might be resulted from pressure broadening. It comes from the fact that nearby particles will affect the radiation emitted by an individual particle. As a result, the spectrum is broader and the cell would seem to be hotter than it actually is.
- Our experiment assumes that the intensities of the transmitting and monitor laser are the same at low-temperature limit of the tellurium cell. The case might not be true since each path goes through different set of optical equipment. The problem could be resolved if the conversion factor were measured at low-temperature limit of tellurium cell and took it into account in Eq.1 by replacing I_0 with αI_0, when α is the conversion factor.

- According to the data from Cariou and Luc's book, there are two other lines close to our considering range with wavenumber 20775.5045 cm^{-1} and 20776.1814 cm^{-1}. These two other lines could have affected the width of the two lines in our consideration. As also shown in Fig. 20, spectroscopy at different temperature does not converge to the same level on the edge of the plot. This can be interpreted as the influence of the nearby lines outside our range of consideration.
- The less likely case that can happen might be that thermocouple wires did not measure the right temperature and the temperature inside the tellurium cell is actually hotter than it indicates on the temperature controller.

5. Reference

Toptica tunable diode laser. (2009, 5). Retrieved from Toptica: http://www.toptica.com/uploads/media/toptica_BR_tunable_diode_lasers_2009_05.pdf

A. Traverso et al. (2009). Inelastic and elastic collision rates for triplet states of ultracold strontium. *Phys. Rev. A 79, 060702(R)*.

Berger, L. I. (1997). *Semiconductor Materials.* Florida: CRC Press, Inc.

Born, V. (1782). *Abh. Privatges. v. Bohmen 5.*

Brooks, L. S. (1952). The Vapor Pressures of Tellurium and Selenium. *J. Am. Chem. Soc., 74(1)*, 227-229.

Ceramic Fiber Heaters. (n.d.). Retrieved from Watlow Electric Manufacturing Company: http://watlow.thomasnet-navigator.com/item/ceramic-fiber-heaters/rs-semi-cylindrical-units-embedded-coiled-elements/vs102a06s#

D. S. Hughes and C. Eckart. (1930). The effect of the motion of the nucleus on the spectra of Li I and Li II. *Phys. Rev. Vol. 36*, 694-698.

Demtroder, W. (2008). *Laser Spectroscopy (Vols, 1-2).* Berlin, Germany: Springer-Verlag.

Derevianko, A. (2001). Feasibility of Cooling and Trapping Metastable Alkaline-Earth Atoms. *Phys. Rev. Lett., Vol 87(2), 023002*.

E. L. Raab et al. (1987). Trapping of Neutral Sodium Atoms with Radiation Pressure. *Phys. Rev. Lett., Vol.59, No. 23*, 2631-2634.

Escobar, Y. N. (2010). *Bose-Einstein Condensation of 84Sr.*

Foot, C. J. (2005). *Atomic Physics.* New York: Oxford University Press Inc.

H. J. Metcalf and Peter van der Straten. (1999). *Laser Cooling and Trapping.* New York: Springer-Verlag New York, Inc.

J. C. Hall and J. A. Magyar. (1976). High resolution saturation absorption studies of methane and some methyl-halides. In K. Shimoda, *High-Resolution Laser Spectroscopy* (p. 173). New York: Springer-Verlag Berlin Heidelberg.

J. Carriou and P. Luc. (1980). *Absorption spectrum of tellurium.* Orsay: Laboratoire Aime-Cotton.

J. E. Sansonetti and G. Nave. (2010). Wavelengths, Transition Probabilities, and Energy Levels for the Spectrum of Neutral Strontium (Sr I). *J. Phys. Chem. Ref. Data, Vol.59, No.3, 033103*.

Klappauf. (2002, April). *Strontium term diagram.* Retrieved from Cold atom group at UNS: http://www.kaiserlux.de/coldatoms/Images/srdiagram.jpg

Lide, D. R. (2008). *Handbook of Chemistry and Physics, 89th ed.* New York: Taylor & Francis.

M. Yasuda and H. Katori. (2004). Lifetime Measurement of the 3P2 Metastable State of Strontium Atoms. *Phys. Rev. Lett. 92, 153004*.

N. Poli et al. (2005). Cooling and trapping of ultracold strontium isotopic mixtures. *Phys. Rev. A 71, 061403*.

P. G. Mickelson et al. (2009). Repumping and spectroscopy of laser-cooled Sr atoms using the (5s5p)3P2-(5s4d)3D2 transition. *J. Phys. B: At. Mol. Opt. Phys. 42, 235001*.

Peron, M. (2012). *Development and Use of a Saturated Absorption Spectroscopy Cell for Tuning the Frequency of the Atom-Cooling Laser.*

Phillips, W. D. (1992). Laser Cooling and Trapping of Neutral Atoms. In W. D. E. Arimondo, *Laser Manupulation of Atoms and Ions* (p. 289). Amsterdam: North-Halland.

S. B. Nagel et al. (2003). Magnetic trapping of metastable 3P2 atomis strontium. *Phys. Rev. A 67, 011401*.

S. Stellmer et al. (2009). Bose-Einstein Condensation of Strontium. *Phys. Rev. Lett. 103(20), 200401*.

T. Kurosu and F. Shimizu. (1990). Laser cooling and trapping of calcium and strontium. *Jpn. J. Appl. Phys.,29*, L2127-L2129.

T. Kurosu and F. Shimizu. (1992). Laser cooling and trapping of alkaline earth atoms. *Jpn. J. Appl. Phys. 31*, 908-912.

T. Loftus et al. (2002). Magnetic trapping of ytterbium and the alkaline-earth metals. *Phys. Rev. A, 66, 013411*.

T. P. Dinneen et al. (1999). Cold collisions of Sr*-Sr in a magneto-optical trap. *Phys. Rev. A, 59(2)*, 1216-1222.

X. Xu et al. (2003). Cooling and trapping of atomic strontium. *J. Opt. Spc. Am. B/Vol. 20, No. 5/May 2003*, 968-975.

6. Appendix

6.1 Matlab curve fitting code

Function data_fitting() can be used to curve fit the spectroscopy of tellurium. This function provides Fig. 22 and 23. It can also be used to calculate the values in table in Application section.

```
function [a,b,c] = data_fitting()

close all
clear all
[A,B] = background();
filename = 'Te absorption spectroscopy.xlsx';
sheet = 1;
cell = {'A5:B25','A30:B50','A55:B75','A80:B100'};
T_label = {'T = 423','T = 473','T = 448','T = 400'};
x0 = [3.5e-4 2597 2.5e-4;
    1e-3 2322 7e-4;
    8e-4 2452 4.5e-4;
    1.3e-4 2746 1e-4];

for i = 1:4
    xlRange = cell{i};

    data = xlsread(filename, sheet, xlRange);
    k = data(:,1)-20776; I = data(:,2);
    subplot(2,2,i)
    plot(k,I,'ro')
    hold on
    xlabel('wavenumber - 20776 (cm^-1)')
    ylabel('transmitted intensity (V)')
    title('Spectoscopy of Te at T = 400 C')

    F = @(x,xdata) (B + A*xdata).*exp((-x(1).*exp(-x(2).*(xdata-
0.0432).^2)...
        -x(3).*exp(-x(2).*(xdata-0.0780).^2)).*sqrt(x(2)));

        [x,resnorm,~,exitflag,output] =...
        lsqcurvefit(F,x0(i,:),k,I);

    hold on
    q = linspace(0,0.1,100);
    plot(q,F(x,q))
    hold off

    a(i) = x(2);
    b(i) = x(1);
    c(i) = x(3);
```

```
        title(T_label{i})
    end

    end
```

Function background() can be used to linearly fit the background signal from monitor beam. The function gives out slope and y-interception of the linear regression as A and B where I(k) = A+B*k.

```
function [A,B] = background()

style = {'o','x','*','.'};
color = {'r-','b-','g-','p-'};
filename = 'Te absorption spectroscopy.xlsx';
sheet = 1;
xRange = 'A5:A25';
data = 'J5:M25';
k = xlsread(filename, sheet, xRange)-20776;
I = xlsread(filename, sheet, data);

for i = 1:4
    p = polyfit(k,I(:,i),1); a(i) = p(1); b(i) = p(2); % I = a*k+b
%     plot(k,I(:,i),style{i})%,k,a(i)*k+b(i),color{i})
    hold on
end

A = mean(a);
B = mean(b);
% plot(k,A*k+B,'r-')
title('Graph of transmitted intensity vs wavenumber of laser')
ylabel('transmitted intensity (V)')
xlabel('wavenumber - 20776 (cm^-1)')
legend('423 C','473 C','448 C','400 C','Location','SouthEast')
end
```

6.2 Frequency offset locking scheme

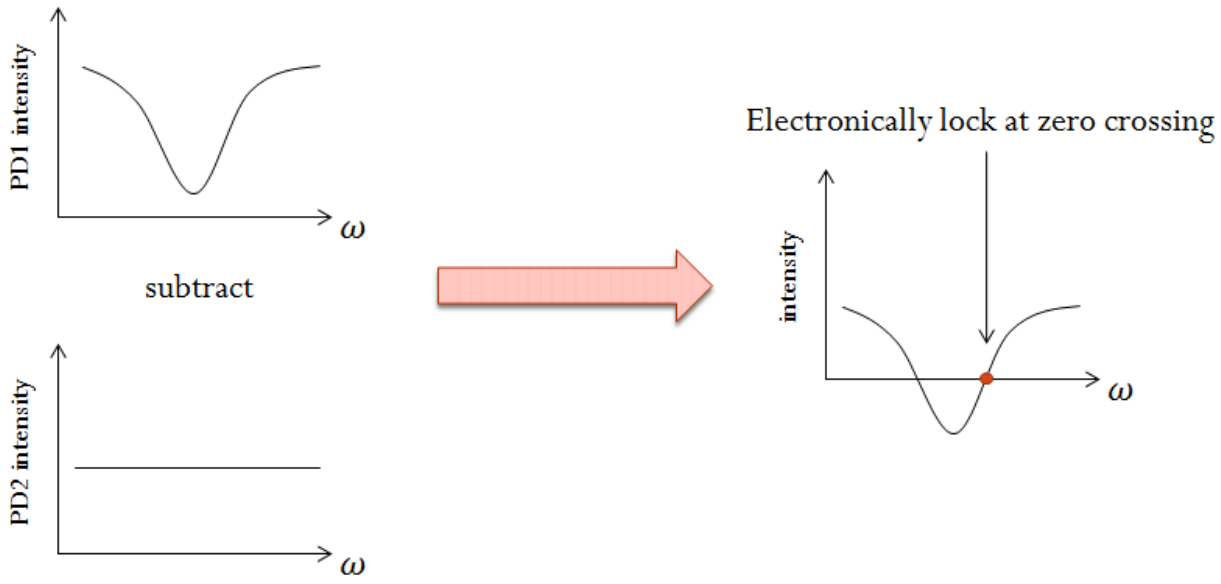

Figure 22: Diagram explaining the frequency offset locking scheme

The wavelength of one of the tellurium lines and that of strontium lines differ only by 48 MHz. The frequency-offset locking technique can be used to lock the 481 nm laser to the side of Doppler broadening of tellurium spectrum. According to the setup from Fig. 8, the signal from each photodiode should be similar to those in Fig. 22. If the signal from PD2 is subtracted from the signal in PD1, the result would be the graph on the right hand side. The complimentary electronics can be constructed to send a feedback to the laser to lock its frequency at the zero crossing point in the intensity and angular frequency graph. If the knob is added into PD2 to adjust the offset, the resultant graph can be shifted upward/downward to select the desired frequency to lock the laser at.

6.3 Absorption cell

The tellurium cell must be heated to a very high temperature for sufficient vapor pressure inside the cell. The vapor pressure and the density of the tellurium gas inside the cell are related through ideal gas law $PV = n_{Sr}KT$. Increasing the temperature of the cell can cause it to absorb

more photons from the laser shining through. In Absorption spectrum of tellurium isotope 120 (J. Carriou and P. Luc, 1980), the well-measured spectrum was taken at 650 ℃, so our goal in heating the oven is to get close to that point.

To prepare for heating up the tellurium cell, a metal insert piece was designed and constructed to hold the tellurium cell inside the oven. The objective of the metal piece was to hold the cell and to evenly distribute heat throughout the cell. Copper is a good candidate as a material used because its melting point is much higher than the 650 ℃ and it is inexpensive.

The cell is made up of two components: body and cap. The body includes a cavity of the size of tellurium cell. A hole of diameter 0.50 inch is drilled in both parts for laser to pass through. Two holes though are offset by 1/8 inch to avoid reflection. On a side of both parts, there is a groove for thermocouple wires to meet at the center of the cell. At the center, a 4-40 tapped hole is located to hold two wires. Two parts are attached with three 10-32 tapped bolts. Due to shape of the tellurium cell, a cut-through groove of length 2.27 inches from the front is required in the body part. The copper cell is made from a copper cylinder of radius 2.00 inches, which is roughly the size of cavity in the oven. It is important to take thermal expansion of copper into an account, because it will be heated to approximately 600 kelvin. For $\alpha_{\mathrm{Cu}} = 16.6 \times 10^{-6}\mathrm{K}^{-1}$, the change in length of the copper cell after being heated can be estimated. Since the length of cavity inside the oven is 6.00 inches,

$\Delta L = L_0 \alpha \Delta T \sim (6 \text{ inches})\left(16.6 \times 10^{-6}\mathrm{K}^{-1}\right)(600 - 300 \text{ K}) = 0.03$ inch. As a result, 0.03 inch should be included when design the length of copper cell. Furthermore, the copper cell is designed to be even shorter to make room for thermocouple wires to bend out. In the end, the total length of copper cell is set to be 5.9 inches to take those two factors into an account.

Below is the CAD drawing of the copper cell.

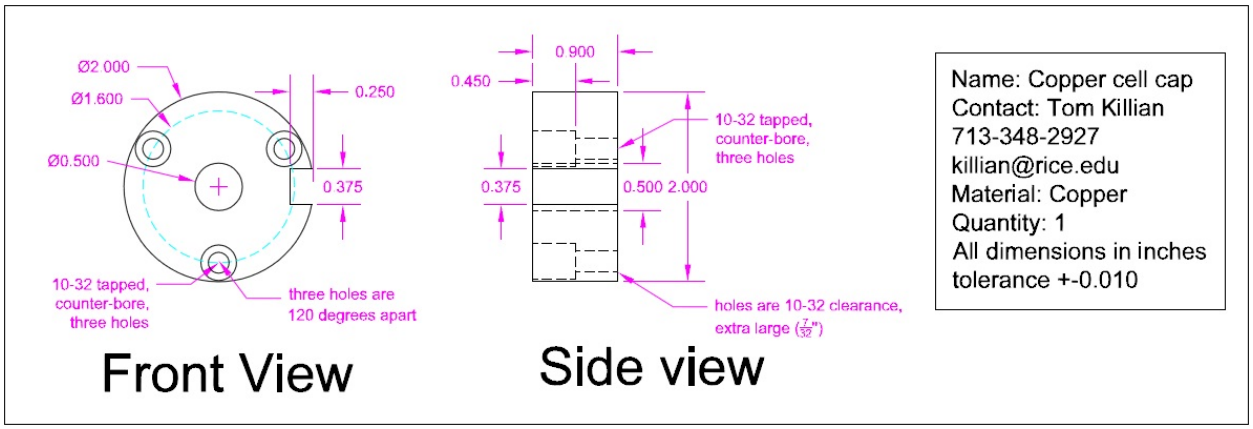

Figure 23: CAD drawing for copper cell cap

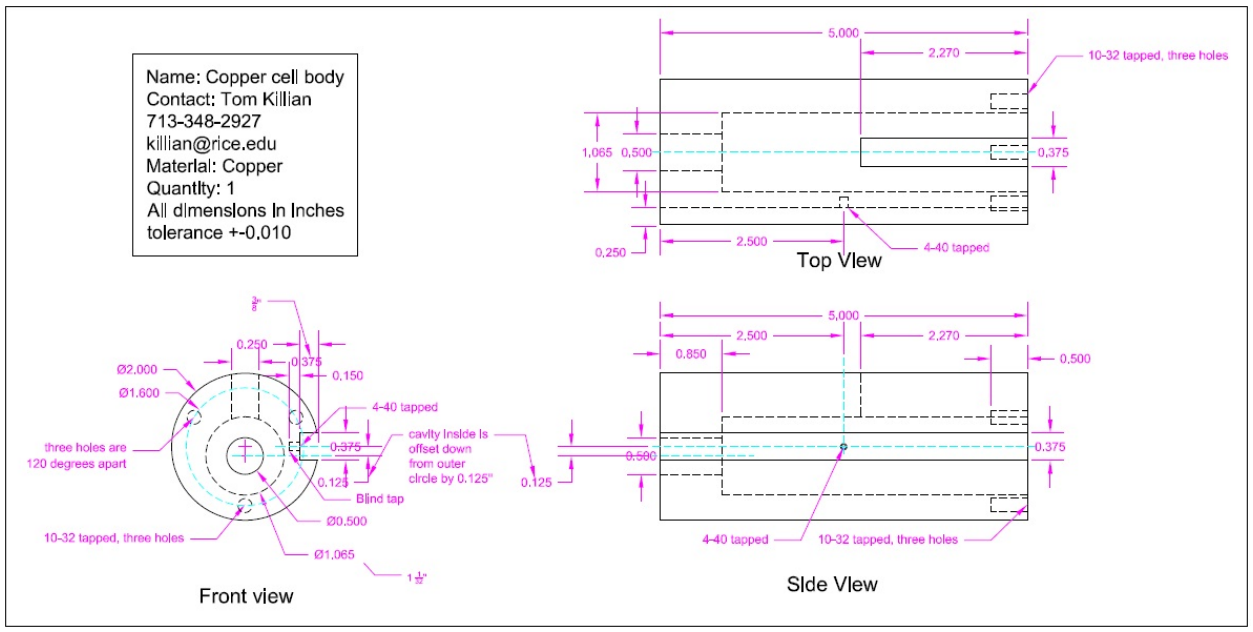

Figure 24: CAD drawing for copper cell body

The drawing was then sent to machine shop and made. The finished parts came back three weeks later. Below is the picture of finished copper cell.

Figure 25: Finished piece of copper cell

Unfortunately, in preliminary tests heating the copper to 700 °C, which was the expected required temperature range because of the vapor pressure curve of tellurium, the cell had problems. As a result of heating up copper insert, the cell “bled” out some other kind of metal as shown in Fig. 26. Evidently the copper was not pure. The amount of alloy bleeding out was quite surprising and unexpected. Several attempts of cleaning the copper piece by heating it up at a high temperature were tried, but were unsuccessful. The amount of alloy bleeding out did not seem to decrease with the time we were willing to spend on this. Furthermore, the metal alloy proved dangerous for our fragile oven.

Figure 26: As a result of heating up copper insert, the cell bled out other kind of metal alloy, as shown above as black fragile layer covering the oven and the copper cell

Consequently, the copper insert was not used in the experiments. Instead of copper insert, layers of fiberglass are used to hold the tellurium cell inside the oven. The stability of motion and the temperature distribution of the tellurium cell were found to be acceptable, and the absorption spectroscopy worked well, as described in the thesis.